Stem Cell Research 17 (2016) 367–378

Contents lists available at ScienceDirect

Stem Cell Research

journal homepage: www.elsevier.com/locate/scr

Tbx3 fosters pancreatic cancer growth by increased angiogenesis and activin/nodal-dependent induction of stemness

Lukas Perkhofer [a], Karolin Walter [a], Ivan G. Costa [b], Maria C. Romero Carrasco [a], Tim Eiseler [a], Susanne Hafner [c], Felicitas Genze [c], Martin Zenke [d], Wendy Bergmann [a], Anett Illing [a], Meike Hohwieler [a], Ralf Köhntop [a], Qiong Lin [d], Karl-Heinz Holzmann [e], Thomas Seufferlein [a], Martin Wagner [a], Stefan Liebau [f], Patrick C. Hermann [a,*], Alexander Kleger [a,*], Martin Müller [a]

[a] Department of Internal Medicine I, Ulm University, Ulm, Germany
[b] IZKF Computational Biology Research Group, Medical Faculty, RWTH University Aachen, Germany
[c] Institute of Pharmacology of Natural Products and Clinical Pharmacology, Ulm University, Ulm, Germany
[d] Department of Cell Biology, Institute for Biomedical Engineering, Medical Faculty, RWTH University Aachen, Germany
[e] Core Facility Genomics, Medical Faculty, Ulm University, Ulm, Germany
[f] Institute of Neuroanatomy, Eberhard Karls University Tuebingen, Tuebingen, Germany

ARTICLE INFO

Article history:
Received 23 December 2015
Received in revised form 5 July 2016
Accepted 8 August 2016
Available online 10 August 2016

Keywords:
TBX3
Pancreas
Pancreatic adenocarcinoma
Development
Cancer stem cells

ABSTRACT

Cell fate decisions and pluripotency, but also malignancy depend on networks of key transcriptional regulators. The T-box transcription factor TBX3 has been implicated in the regulation of embryonic stem cell self-renewal and cardiogenesis. We have recently discovered that forced TBX3 expression in embryonic stem cells promotes mesendoderm specification directly by activating key lineage specification factors and indirectly by enhancing paracrine NODAL signalling. Interestingly, aberrant TBX3 expression is associated with breast cancer and melanoma formation. In other cancers, loss of TBX3 expression is associated with a more aggressive phenotype e.g. in gastric and cervical cancer. The precise function of TBX3 in pancreatic ductal adenocarcinoma remains to be determined. In the current study we provide conclusive evidence for TBX3 overexpression in pancreatic cancer samples as compared to healthy tissue. While proliferation remains unaltered, forced TBX3 expression strongly increases migration and invasion, but also angiogenesis *in vitro* and *in vivo*. Finally, we describe the TBX3-dependency of cancer stem cells that perpetuate themselves through an autocrine TBX3–ACTIVIN/NODAL signalling loop to sustain stemness. Thus, TBX3 is a new key player among pluripotency-related genes driving cancer formation.

1. Introduction

Pancreatic ductal adenocarcinoma (PDAC) remains one of the most lethal malignancies in the western world (Jemal et al., 2010). Due to an increasing incidence it is estimated to be the third leading cause of cancer-related deaths by 2030 (Rahib et al., 2014). While overall survival in many solid malignancies has significantly improved over the last decade (Jemal et al., 2010), there has only been a marginal improvement in PDAC despite improved therapies and surgical techniques (Howlader et al., 2013). At diagnosis, only 15–20% of the patients even qualify for potentially curative resection. Most patients present with already locally advanced or metastatic disease, caused by the usually late diagnosis due to missing early symptoms and early metastatic spread, a hallmark of PDAC (Haeno et al., 2012). 5-year survival ranges around 7% (Jemal et al., 2010; Howlader et al., 2013), and even after surgical resection and subsequent state-of-the-art adjuvant chemotherapy, the overall survival rate does not exceed 20% (Jemal et al., 2010; Haberland et al., 2010). Regrettably few patients survive longer, but the distinguishing features that predict long-term survival are not yet fully understood (Yachida et al., 2012; Russell et al., 2015a). It has been demonstrated that virtually all cancers including PDAC are highly heterogeneous and contain a subset of cancer stem cells, tumour cells with features that distinguish them from the tumour bulk (Al-Hajj et al., 2003; Hermann et al., 2007; Kim et al., 2005; Li et al., 2007; O'Brien et al., 2007; Ricci-Vitiani et al., 2007; Singh et al., 2004). These tumour cells can self-renew, have an exceptionally high tumour-initiating capacity, and recapitulate the heterogeneity of the parental tumour. Furthermore, these cells have distinct metabolic (Sancho et al., 2015) and cell cycle properties, are highly chemoresistant (Cioffi et al., 2015; Mueller et al., 2009; Hermann et al., 2013; Hermann et al., 2007), and are responsible for metastatic spread (Hermann et al., 2007). Finally, these cells contain

* Corresponding authors at: Department of Internal Medicine I, Ulm University, Albert-Einstein-Allee 23, 89081 Ulm, Germany.
E-mail addresses: patrick.hermann@uni-ulm.de (P.C. Hermann), alexander.kleger@uni-ulm.de (A. Kleger).

http://dx.doi.org/10.1016/j.scr.2016.08.007

a self-renewal machinery driven by up-regulated pluripotency factor expression such as NANOG or OCT3/4 and by re-activation of embryonic pathways such as NODAL/ACTIVIN signalling (Lonardo et al., 2011). Thus, these pancreatic cancer stem cells share certain stemness features with bona fide pluripotent embryonic stem cells (Liebau et al., 2014).

The T-box transcription factor 3 (TBX3) belongs to an ancient group of genes that share a highly conserved DNA binding domain, the T-box (Muller and Herrmann, 1997; Minguillon and Logan, 2003; Bertolessi et al., 2015; Weidgang et al., 2016). TBX3 is widely expressed in many tissues, plays a pivotal role during embryonic development, and is tightly linked to early lineage commitment and the pluripotency of embryonic stem cells (Kim et al., 2008; Weidgang et al., 2013; Kartikasari et al., 2013; Russell et al., 2015b; Waghray et al., 2015). Furthermore, TBX3 functions as a transcriptional repressor, is implicated in cell cycle regulation, and in tumour development. TBX3 is overexpressed in human colorectal (Shan et al., 2015), head and neck (Burgucu et al., 2012), bladder (Beukers et al., 2015) and breast cancer (Fan et al., 2004; Yarosh et al., 2008) as well as in melanoma (Peres et al., 2010). Most recently, high TBX3 expression has been shown to negatively correlate with survival in a cohort of 80 resected human PDAC samples (Wang et al., 2015), demonstrating a substantial role of TBX3 in pancreatic cancer. Moreover, TBX3 overexpression was found to be a negative prognostic factor in colorectal cancer (Shan et al., 2015) and hepatocellular carcinoma (Renard et al., 2007). Mechanistically, TBX3 is repressed by miR-206 and miR-17-92 to inhibit proliferation but also to decrease the cancer stem cell population in breast and pancreatic cancer (Cioffi et al., 2015; Amir et al., 2016), while in certain sarcomas it drives proliferation via p21 repression. Its expression qualifies as a biomarker to predict survival (Willmer et al., 2016a; Willmer et al., 2016b). Interestingly, putative cancer driver mutations in the TBX3 gene cause impaired transcriptional repression in breast cancer (Fischer and Pflugfelder, 2015) and correlate with an invasive lobular carcinoma phenotype (Ciriello et al., 2015). Therefore, targeting TBX3 itself or its signalling axis may be of high clinical relevance in the future.

In this study, we aim to close a gap of knowledge determining the precise function of TBX3 in pancreatic ductal adenocarcinoma. In contrast to other cancers, we found TBX3 to be overexpressed in human PDAC, driving invasion and stemness. Specifically, TBX3 seems to activate key genes driving angiogenesis but also sustaining NODAL/ACTIVIN signalling.

2. Material and methods

2.1. Cell culture and MTT assay

Pancreatic cancer cells were grown in DMEM or RPMI, supplemented with 10% fetal calf serum and 1% Penicillin/Streptomycin. Cells were grown at 37 °C in a humidified atmosphere with 5% CO_2. Passages used for experiments ranged from passage 15 to 32.

For cell treatment 10.000 cells/well were seeded in 96 well plates and grown for 24 h. Following capecitabine (Roche), gemcitabine (Fresenius Kabi) and cisplatin (Sigma-Aldrich; P4394) were added in the dosages as referred to in the text. After 24 h, treated cells were washed with PBS and MTT (Sigma-Aldrich; M2128) was added for 3 h to allow metabolization. Finally, DMSO was added and readout followed by measuring optical density at 560 nm.

2.2. Lentiviral transduction for stable TBX3 overexpression

Human TBX3 cDNA was lentivirally overexpressed using a pLenti6.2/V5 backbone as described in (Fillmore et al., 2010). pLentiviral particles were produced according to standard protocols using psPax2 and pMD2 (Addgene; #12260, #12259) as packaging plasmids in LentiX HEK293T cells (Clontech). Cells were infected directly with LentiX HEK293T supernatant for 8 h at 37 °C. 24 h later, blasticidine selection was performed at a concentration of 10 μg/ml for 7 days.

2.3. Immunohistochemistry of human PDAC samples

Human PDAC tissue microarrays were obtained from a commercial supplier (BIOMAX US). Immunohistochemical analysis was performed on the section (Pa1001a using the biotin/streptavidin peroxidase LSAB kit (Vector Labs). After microwave (20 min) antigen retrieval (citrat based antigen-retrieval solution pH .0; Dako), an antibody against TBX3 (Abcam; ab89220) was applied at room temperature, followed by application of the biotin/streptavidin reagents according to the manufacturer's instructions. For Ki67 visualization, anti-Ki67 (Abcam; ab15580, 1:500) antibody was incubated overnight at 4 °C. Tissues were analyzed and photographed using a Leica stereomicroscope. For the quantification of the immunohistochemistry stainings 10 randomly selected high power fields were counted, at 40× magnification, per slide. Immunohistochemistry and quantification of CAM-derived tumours were performed similarly. Antibodies used in the CAM were anti-human Desmin Clone33 (Dako; M0760, 1:100), anti-VEGF (Abcam; ab1316, 1:100) and anti-Cytokeratin (CAM 5.2 = CK8) (BD Biosciences; #349205, 1:10), Ki67 (Dako; M7240, 1:80), Vimentin (Dako; M5020, 1:300), Cytokeratin AE1/AE3 (Dako; M3515, 1:80). TUNEL staining: *In situ* cell death detection kit, POD (Roche; #11684817910).

2.4. Immunofluorescence staining

Human pancreatic cancer cells were washed in PBS and then fixed in 4% Paraformaldehyde (PFA). Samples were then treated with NH_4Cl and blocked with 0.1% Triton-X-containing BSA before incubation with the primary antibodies: Mouse antibody against TBX3 (Abcam; ab89220), dilution 1:50, for 2 h at room temperature and mouse anti-OCT-3/4 (Santa Cruz Biotechnology; sc-9081), dilution 1:10 for 2 h at room temperature. Subsequently, the samples were incubated with fluorescent labelled secondary antibodies Alexa Fluor® 488 (green), Alexa Fluor® 568 (red), Alexa Fluor® 647 (magenta) (Life-technologies, all diluted 1:500). Nuclei were stained with DAPI (blue) (1:5000). Images were captured using a Leica TCS SP8-HCS confocal microscope, 63× Plan Apo Water emersion objectives. Images were acquired in sequential scan mode and represent single confocal airy sections.

2.5. Sphere formation assay

Pancreatic cancer spheres were generated as described previously (Hermann et al., 2013) and cultured in DMEM-F12 (Invitrogen) supplemented with B-27 (Gibco), basic fibroblast growth factor (PeproTech EC) and heparin (Braun). 15.000 cells/ml were seeded in ultra-low attachment plates (Corning B.V.). Spheres were defined as 3-dimensional multicellular structures of approximately 40 μm or larger. Sphere formation was quantified manually using a Leica stereomicroscope. Inhibition of ALK was conducted with SB431542 (ESI BIO).

2.6. Flow cytometry

FACSorting was performed as described previously using CD133/1-PE (Miltenyi Biotech) and EpCAM-APC (BD Bioscience) antibodies (Hermann et al., 2008). DAPI (eBiosciences) was used to exclude dead cells. Samples were sorted using a FACS Aria II cell sorter (BD Bioscience). FACS Apoptosis analysis was performed by using a FITC Annexin V Apoptosis detection kit with 7-AAD (BioLegend) as specified by the manufacturer. For BRDU staining a FITC Mouse Anti-BrdU antibody (BD Bioscience; #347583 CloneB44) and propidium iodide were used. The distribution of apoptotic cells and cell cycle phases were quantified by BD FACS DIVA software (BD Biosciences) analysis.

2.7. Transmigration, proliferation and invasion assays

Transwell migration assays using stably transfected TBX3-OE or TBX3-SCR BxPC3 and Panc1 cells were performed according to standard methods as previously described (Eiseler et al., 2012).

2.8. Quantitative real-time PCR and Western blot analysis

Immunoblotting was performed according to standard procedures as described previously (Kleger et al., 2010; Kleger et al., 2012). Primary antibodies were as follows: TBX3 antibody (Abcam; ab89220, 1:100) and β-Actin (Sigma-Aldrich; A2228, 1:1000) .

2.9. CAM assay

CAM assays have been described previously (Azoitei et al., 2011; Muller et al., 2015). Briefly, shells of fertilised chicken eggs were opened on day 5 and silicon rings (5 mm in diameter) were applied onto the chorioallantoic membrane (CAM). On day 8 after fertilisation, 1×10^6 cells (BXPC3 and PANC1, TBX3-OE or scrambled controls) suspended in 20 μl DMEM/Matrigel (1:1, v/v) were transplanted. After 72 h tumours were harvested and photographed. Tumour size was calculated after measuring two diameters, n ≥ 4 CAMs per cell line.

2.10. Regulatory genomics analysis

TBX3 ChIP-Seq and control experiments on mouse ES cells (Waghray et al., 2015) were obtained in Gene Expression Omnibus (GSE60066). Reads were mapped to mouse mm9 genome using BWA (Li and Durbin, 2009) and peak calling was performed with MACS (Zhang et al., 2008) by providing both IP and control signals and a false discovery rate (FDR) of 0.2 Gene enrichment analysis was performed on TBX3 peaks with GREAT (Zhang et al., 2008) (PMID 20436461). We only report gene sets associated to TGFβ, NODAL and ACTIVIN, which obtained an adjusted p-value <0.05 with the Binomial test.

2.11. Statistical analysis

Results for continuous variables are presented as means ± SEM of 3 independent experiments unless stated otherwise. To test for statistically significant differences, nonparametric Mann–Whitney-U testing was performed using GraphPad Prism 6 software (GraphPad, San Diego, CA). Differences were considered statistically significant at either * $p < 0.05$, ** $p < 0.01$ or *** $p < 0.001$.

3. Results

3.1. TBX3 is overexpressed in human PDAC

TBX3 overexpression has been reported for several cancers and usually predicts poor outcome and more invasive properties (Shan et al., 2015; Wang et al., 2015). We screened published microarray datasets for gene expression analyses of PDAC and healthy tissues (Gadaleta et al., 2011) and were able to confirm an increased expression of TBX3 in PDAC as compared to either normal tissue adjacent to PDAC or to tissue from healthy donors (Fig. 1A; http://www.pancreasexpression.org/). To extend these findings we determined *TBX3* expression levels via qPCR in a set of resected human primary tumours and corresponding normal pancreatic tissue samples. *TBX3* was strongly overexpressed in cancer samples as compared to non-tumour tissue (Fig. 1B). To confirm these findings on the protein level, we assessed TBX3 expression via immunohistochemistry in tissue microarrays (55 PDAC samples, 17 normal tissue). While in healthy acinar and ductal tissue TBX3 expression was very weak or absent, various PDAC samples showed a pronounced nuclear TBX3 positivity (Fig. 1C-E and Supp. Fig. 1). Out of 55 tumours, 47 were classified as positive and only 8 as negative for TBX3 (Table 1). Interestingly, the staining was heterogeneous within individual tumours and sometimes revealed only few highly TBX3-positive nuclei, suggesting a role of TBX3 in a subpopulation of tumour cells. While we could not observe a direct correlation between tumour stage and TBX3 expression (Table 1), the high number of TBX3-positive tumors clearly suggests that TBX3 expression is closely linked to pancreatic tumour development.

3.2. TBX3 expression has no effect on proliferation or apoptosis in human pancreatic cancer cells

We measured *TBX3* levels in established pancreatic cancer cell lines (Panc1, BxPC3) and found only low *TBX3* expression as demonstrated via qPCR and immunoblotting (Figs. 2A–C). To determine whether TBX3 alone is sufficient to promote oncogenic properties in human pancreatic cancer, we stably overexpressed TBX3 in these cell lines using a lentiviral overexpression construct (Figs. 2A–C). Interestingly, overexpression of TBX3 had no influence on the proliferation of pancreatic cancer cells as compared to controls resulting in almost identical growth curves (Fig. 2D and Supp. Fig. 2C). While we could not detect relevant differences in cell cycle distribution, apoptosis was slightly lower in TBX3-overexpressing (TBX3-OE) cells as demonstrated by BrdU- and AnnexinV/7AAD assays (Supp. Fig. 2A,B,D,E). To evaluate the role of TBX3 during cellular stress, we cultured these cells with the standard chemotherapeutic agents capecitabine, cisplatin and gemcitabine, as well as under hypoxia and serum starvation. However, there was no significant difference in proliferation between TBX3-OE and scrambled control (TBX3-SCR) cells (Fig. 2G,H and Supp. Fig. 3A–D).

3.3. TBX3 drives migration, invasion and sphere formation in human pancreatic cancer cells

High proliferation rates, resistance to environmental stress and chemotherapy are hallmarks of tumour development and aggressiveness. Further key factors are migration and invasion of tumour cells, ultimately resulting in metastasis. Indeed, TBX3 has been shown to mediate these features in other cancers (Peres et al., 2010; Li et al., 2013; Mowla et al., 2011). Therefore, we focused on these aspects of tumour development and evaluated the TBX3-OE cell lines in a series of *in vitro* migration and invasion assays. Intriguingly, overexpression of TBX3 resulted in significantly enhanced migration (Fig. 2E and Supp. Fig. 3E) and invasion (Fig. 2F and Supp. Fig. 3F) in both investigated pancreatic cancer cell lines. Migration and invasion are usually preceded by epithelial-to-mesenchymal transition (EMT), which in turn links stemness and anchorage-independent growth in cancer (Rhim et al., 2012). In contrast to other tumours (Boyd et al., 2013), we could not observe EMT features in TBX3-OE cells using qPCR analysis for typical marker genes (data not shown). In line with our qPCR data, TBX3 overexpression did not induce EMT as shown by vimentin staining in the epithelial BxPC3 cells. In contrast, Panc1-derived tumours expressed vimentin in the cytoplasm of the tumour cells, indicative of a more mesenchymal state of these cells. However, overexpression of TBX3 did not alter vimentin expression in these cells. To more globally assess increased migration and invasion triggered by TBX3, we used Genomic Regions Enrichment of Annotations Tool (GREAT) (http://great.stanford.edu/public/html/index.php) analysis based on published TBX3-ChIP-sequencing. GREAT associates genomic regions with genes by defining a 'regulatory domain' for each gene in the genome (Waghray et al., 2015). We have selected out of the significantly enriched terms from TBX3-bound genes, all GO Terms with either "cytoskeleton", "focal adhesion", "migration" and "metastasis" in their description. This indicates an involvement of TBX3 in both cell migration and metastasis formation (Fig. 2J).

Finally, we assessed the influence of TBX3 overexpression on a putative cancer stem cell population. We performed sphere formation assays

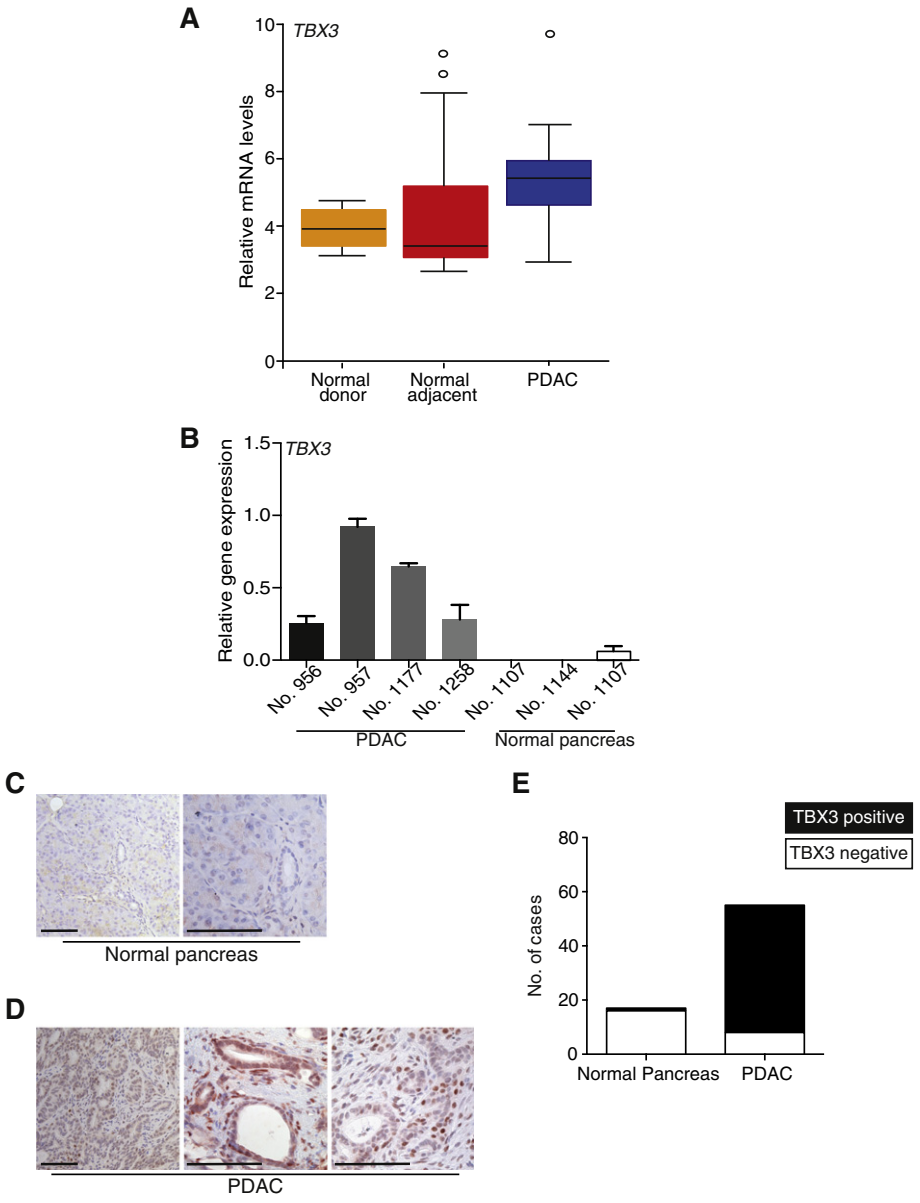

Fig. 1. Increased TBX3 expression in human pancreatic ductal adenocarcinomas. (A) Tbx3 expression based on microarray analysis. Data were taken from www.pancreaticexpression.org and are based on Gadaleta et al. (2011). (B) qRT-PCR analysis of *TBX3* expression, showing increased levels in human PDAC samples compared to healthy pancreatic tissue. Data are represented as relative gene expression of TBX3 and normalized to *HMBS*. Representative pictures of TBX3 immunohistochemistry in (C) healthy pancreatic tissue and (D) in different representative PDAC samples. Scale bars: 50 μm. (E) Quantification of TBX3 protein expression in a human tissue microarray referring to Table 1. (n ≥ 3 for all experiments).

and observed that TBX3-OE cells formed spheres at a significantly higher efficiency (Fig. 2I). Thus we conclude that TBX3 expression does not affect proliferation but drives invasion and migration, and promotes sphere formation of human pancreatic cancer cells *in vitro*.

3.4. TBX3 overexpression drives angiogenesis and tumour expansion in vivo

To investigate pro-tumourigenic effects of TBX3 we performed xenotransplantation experiments using a chicken chorioallantoic membrane (CAM) assay that faithfully mimics *in vivo* tumour growth (Muller et al., 2015; Azoitei et al., 2014; Azoitei et al., 2012; Azoitei et al., 2010). TBX3 overexpressing BxPC3 and Panc1 cells were transplanted on the surface of the CAM 8 days after fertilization, and xenograft tumour formation was observed, measured, and analysed by immunohistochemistry (IHC) after 72 h (Fig. 3A). Both macroscopically and microscopically the tumours generated from TBX3-OE cells were significantly larger than tumours induced by control cells (Fig. 3B–D,F). In line with our *in vitro* data, Ki67 staining was similar in both groups (Fig. 3E,G–I). Furthermore, TUNEL-staining did not show significant differences in apoptosis between TBX3-OE and SCR tumours, albeit there was a trend towards fewer apoptotic cells in the TBX3 gain of function groups (Supp. Fig. 4A,B). Of note, TBX3-OE tumours appeared to be remarkably more invasive than control tumours, with increased scattered tumour islets, almost penetrating the CAM (Fig. 3B,C; insert). We then characterized the arising tumours via IHC: Expression of the ductal marker CK19 was independent of TBX3 expression (Fig. 3H,I). Interestingly, visualisation of the exclusively human tumour cell derived tissue on the CAM by specific staining for human CK8 illustrates bigger and more tumour cell clusters indicative for a higher tumour-initiating capacity of the TBX3-overexpressing cells (Supp. Fig. 4C). Next, we aimed to investigate EMT *in vivo* in the context of TBX3 expression. Vimentin fibres were exclusively deposited in the tumour stroma in the BxPC3 cells while the Panc1 cells showed baseline positivity for vimentin indicating a mesenchymal fate in the Panc1 without further

Table 1
Pancreatic cancer cohort (commercial TMA).

Characteristics		All	%	TBX3 pos	%	TBX3 neg	%
		55	100	47	85,5	8	14,5
Sex							
	Male	31	56,4	27	87,1	4	12,9
	Female	24	43,6	20	83,3	4	16,7
Age		58,7		58,9		57,8	
	(Range)	(38–80)		(38–80)		(46–76)	
T-Category							
	T1	-		-		-	
	T2	23	41,8	21	44,7	2	25,0
	T3	30	54,5	25	53,2	5	62,5
	T4	2	3,6	1	2,1	1	12,5
N-Category							
	NO	44	80,0	36	76,6	8	100,0
	N1 +	11	20,0	11	23,4	-	
M-Stage							
	M0	51	92,7	43	91'5	8	100,0
	M1	4	7,3	4	8,5	-	
Stage grouping							
	I	21	38,2	19	40,4	2	25,0
	II	28	50,9	23	48,9	5	62,5
	III	2	3,6	1	3,7	1	25,0
	IV	4	7,3	4	14,8	-	
Differentiation		n = 53					
	Grade 1	8	15,1	7	17,8	1	12,5
	Grade 2	30	56,6	26	66,7	4	50,0
	Grade 3	15	28,3	12	33,3	3	37,5

TBX3 staining was confirmed as positive when there was at least 1% nuclear labelling within the cell fraction.

impact of TBX3 overexpression in both cell types. No obvious difference was observed between both groups regarding stroma content (Fig. 3H,I).

Interestingly, TBX3-overexpressing tumours showed significantly enhanced angiogenesis. Both, increased expression of angiogenesis-associated genes (*FGF2/VEGF-A*) as well as increased desmin and VEGF-A positive structures were detected in TBX3-overexpressing tumours (Fig. 3 J–M). This observation is further supported by GREAT analysis in ChIP-seq data. Here the terms "VEGF-signalling" or "Signalling events mediated by VEGFR1 and VEGFR2" are among the significantly enriched terms (Fig. 3N). In summary, TBX3 expression enhances tumour growth and CAM invasion *in vivo* via increased angiogenesis and most likely by higher tumour initiation.

3.5. TBX3 promotes a cancer stem cell phenotype in PDAC

In turn, we tried to dissect the underlying mechanism, which seemed to be independent of proliferation, apoptosis and cellular resistance. To investigate this in more detail we followed up on the observation that TBX3 overexpression enhances sphere formation and more tumour cell clusters on the CAM (Fig. 2I; Supp. Fig. 4C). Since this matches previous data that TBX3 promotes pluripotency of embryonic stem cells, we hypothesized that TBX3 expression may promote a cancer stem cell (CSC) phenotype. Of note, sphere formation assays are the gold standard to assess the stemness of tumour cells *in vitro* by selecting for undifferentiated cells that grow in anchorage-independent culture conditions with certain growth factors. Due to their inherent heterogeneity in early passage, primary cancer cells much better reflect the inter-individual differences between tumour patients, and thus represent a far better model system for the investigation of CSCs than long-established cell lines (Hermann et al., 2013). Furthermore, we aimed to investigate the role of endogenous TBX3 in primary tumour cells without overexpression of TBX3. Therefore we extended our investigation to three patient xenograft-derived primary cell lines (Panc354, Panc185, Panc215) that were generated as described previously (Rubio-Viqueira and Hidalgo, 2009; Lonardo et al., 2011). Underpinning the link to CSCs, we found TBX3 to co-localize with the pluripotency-defining factor OCT3/4 in adherent primary cancer cells (Fig. 4A). CSCs are enriched in the $CD133^+$ subpopulation and in sphere cultures (Hermann et al., 2007; Lonardo et al., 2011). We therefore sorted the primary PDAC cell lines for CD133 and could confirm a significantly increased mRNA expression of the stemness gene *NANOG* and *TBX3* in $CD133^+$ cells (Fig. 4B). Furthermore, we were able to show highly positive TBX3 staining in the $CD133^+$ cells in contrast to a virtual absence in the $CD133^-$ population (Fig. 4C).

Interestingly, both in $CD133^+$ cells as well as in spheres, we observed significantly increased *TBX3* levels as compared to control cells ($CD133^-$ or adherent cells, respectively; Fig. 4D,E). Increased *NANOG* and *OCT3/4* expression levels demonstrate elevated stemness in the respective population (Fig. 4D). We have shown previously that TBX3 drives mesendoderm formation via a TBX3 –NODAL–SMAD signalling axis (Weidgang et al., 2013), and NODAL-signalling has been described to be essential for cancer stem cell self-renewal (Lonardo et al., 2011; Lonardo et al., 2012). To shed light on the role of TBX3 expression in cancer stem cells we made again use of the mentioned ChIP-sequencing dataset to identify genes directly bound/regulated by TBX3 (Waghray et al., 2015). Here we identified strongly enriched GO terms in TBX3-bound genes that are involved in "NODAL-, TGFβ-, and ACTIVIN-signalling" as demonstrated in Fig. 5A. Encouraged by this global assessment of pathways driving self-renewal of CSCs (Lonardo et al., 2011), we wondered whether a core set of genes previously reported to be enriched in CSCs are directly bound by TBX3. Indeed, *NODAL*, *INHBB* (subunit of *ACTIVIN A*), *SMAD4* and *ALK4* show overlapping TBX3 binding peaks with DNAse ChIP-sequencing peaks, which is highly indicative for a direct gene activation (Fig. 5B). To confirm these findings we compared expression of these genes in spheres compared to adherent cells in primary pancreatic cancer cells. Indeed, *ACTIVIN A* and *NODAL* as well as their downstream effectors *ALK4* and *SMAD4* were significantly increased in spheres (Fig. 5C). Next, we aimed to causally link *ACTIVIN/NODAL* signalling with *TBX3* expression and found that stimulation of Panc354 cells with recombinant ACTIVIN resulted in increased expression of *TBX3*, *NODAL*, and *ACTIVIN A* itself (Fig. 5D). This strongly suggests that TBX3 is located downstream of the ACTIVIN A signalling cascade and might reinforce ACTIVIN A signalling directly by its own expression. To confirm this hypothesis, we generated TBX3-OE primary pancreatic cancer cells to measure *ACTIVIN A* levels. As expected, TBX3 overexpression resulted in increased levels of *ACTIVIN A*, confirming our hypothesis of increased CSC self-renewal through an autocrine NODAL/ACTIVIN–TBX3–NODAL/ACTIVIN feedback loop (Fig. 5E). Vice versa, selective compound inhibition of the Activin Receptor-like Kinase Receptors 4/5 (ALKs 4/5) with SB431542 significantly repressed the expression of *TBX3* and *ACTIVIN A* (Fig. 5F). Moreover, sphere formation was greatly reduced by treatment with SB431542 (Fig. 5G,H), which is well in line with previous reports (Lonardo et al., 2011).

Taken together, we here postulate that TBX3 enhances tumour growth and aggressiveness via a dual mechanism: Firstly, it increases migratory and invasive properties in the tumour bulk and secondly it induces a cancer stem cell population by increasing stemness features via an autocrine NODAL/ACTIVIN–TBX3–NODAL/ACTIVIN axis (Fig. 6).

4. Discussion

The diagnosis of pancreatic ductal adenocarcinoma still means a dismal prognosis for patients. The highly homologous T-box transcription factor TBX3 is overexpressed in various solid tumours mediating proliferation, EMT, increased invasion/migration, and the ability for cells to bypass senescence (Shan et al., 2015; Burgucu et al., 2012; Beukers et al., 2015; Fan et al., 2004; Yarosh et al., 2008). TBX3 is overexpressed in human PDAC, but its precise role in the development and perpetuation of this tumour remains unclear. However, there is evidence for TBX3 as a promoter of metastasis (Fillmore et al., 2010) and its expression has been linked to EMT, as suggested by TBX3-mediated repression of E-cadherin (Wang et al., 2015; Peres and Prince, 2013). In line with previous data from Wang et al. (Wang et al., 2015) we confirm TBX3

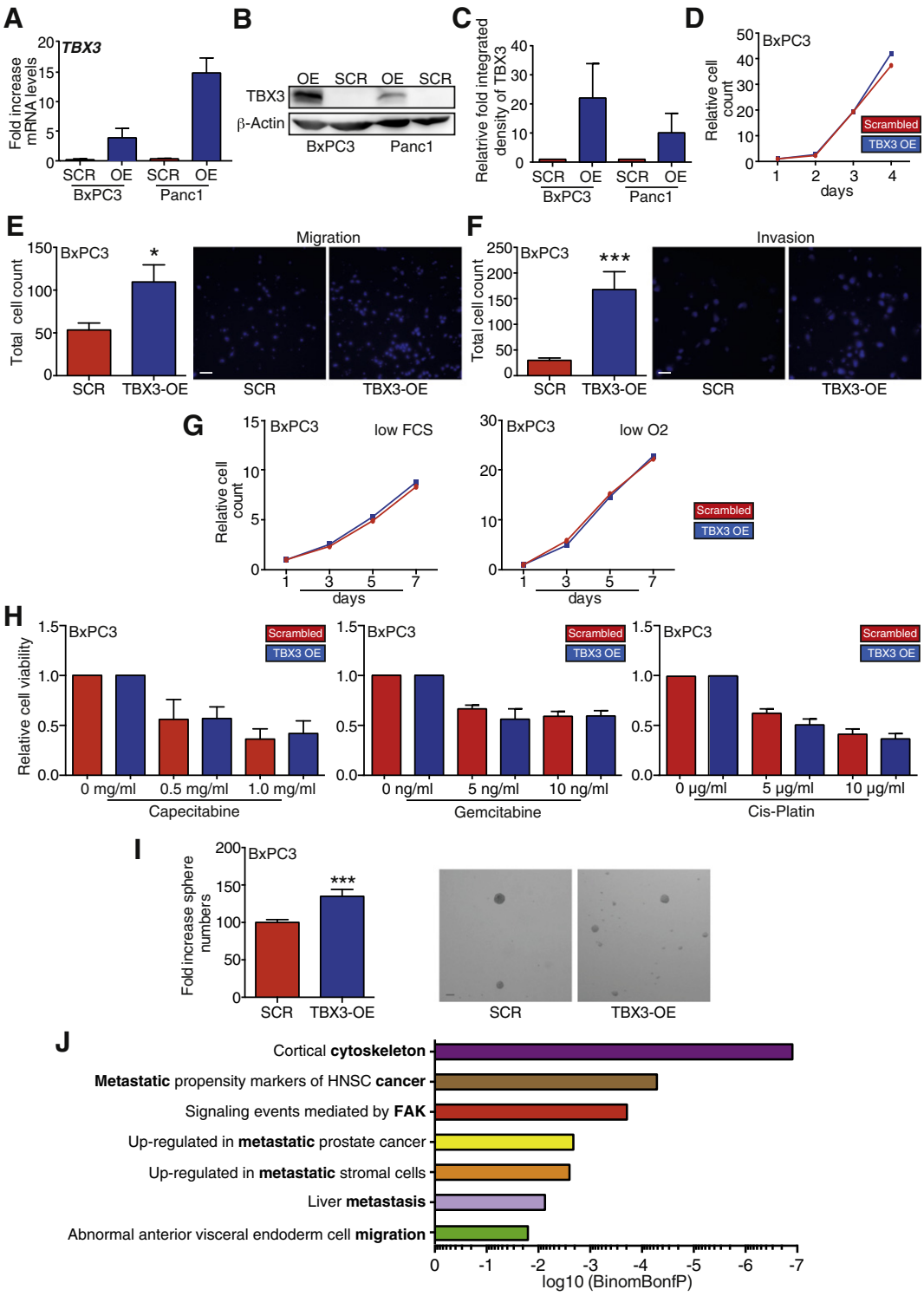

Fig. 2. TBX3 promotes migration, invasion and sphere formation capability of human PDAC cell lines. (A–B) TBX3 expression on mRNA and protein levels for scrambled (SCR) and TBX3 overexpressing (TBX3-OE) human PDAC cell lines (BxPC3, Panc1), measured by qRT-PCR and Western blot. (C) Quantification of relative band intensity from Western blot as fold integrated density of TBX3. (D) TBX3-OE does not increase cell growth in BxPC3 cells. TBX3-OE results in significantly increased (E) migration and (F) invasion of BxPC3 cells. Representative DAPI stained images (20× magnification, scale bars: 100 µm) are provided for all experiments. (G) TBX3-OE does not alter cell numbers in BxPC3 cells under low serum culture (1% FCS), and hypoxic conditions (5% O2) compared to SCR. (H) Sensitivity towards chemotherapy with either capecitabine (0.5–1.0 mg/ml), gemcitabine (5–10 ng/ml) or cisplatin (5–10 µg/ml) is not affected by overexpression of TBX3 in BxPC3 cells. (I) Overexpression of TBX3 escalates sphere formation capability as compared to SCR-control. Representative pictures from BxPC3 sphere cultures after 7 days. Scale bar: 100 µm ($n \geq 3$ for all experiments). (J) Genomic Regions Enrichment of Annotations Tool (GREAT) (http://great.stanford.edu/public/html/index.php) analysis: GREAT associates genomic regions with genes by defining a 'regulatory domain' for each gene in the genome. Listed are all significantly enriched GO terms in TBX3 bound genes with either "cytoskeleton" "focal adhesion" "migration" and "metastasis" in their description.

overexpression in PDAC patient samples when compared to normal pancreatic tissue. For further evaluation of its oncogenic potential we used well-established and well-characterized human PDAC cell lines and overexpressed TBX3. We could not detect relevant changes in proliferation, which is well in line with observations in other solid tumours like melanoma. Interestingly, TBX3 expression even inhibits cell

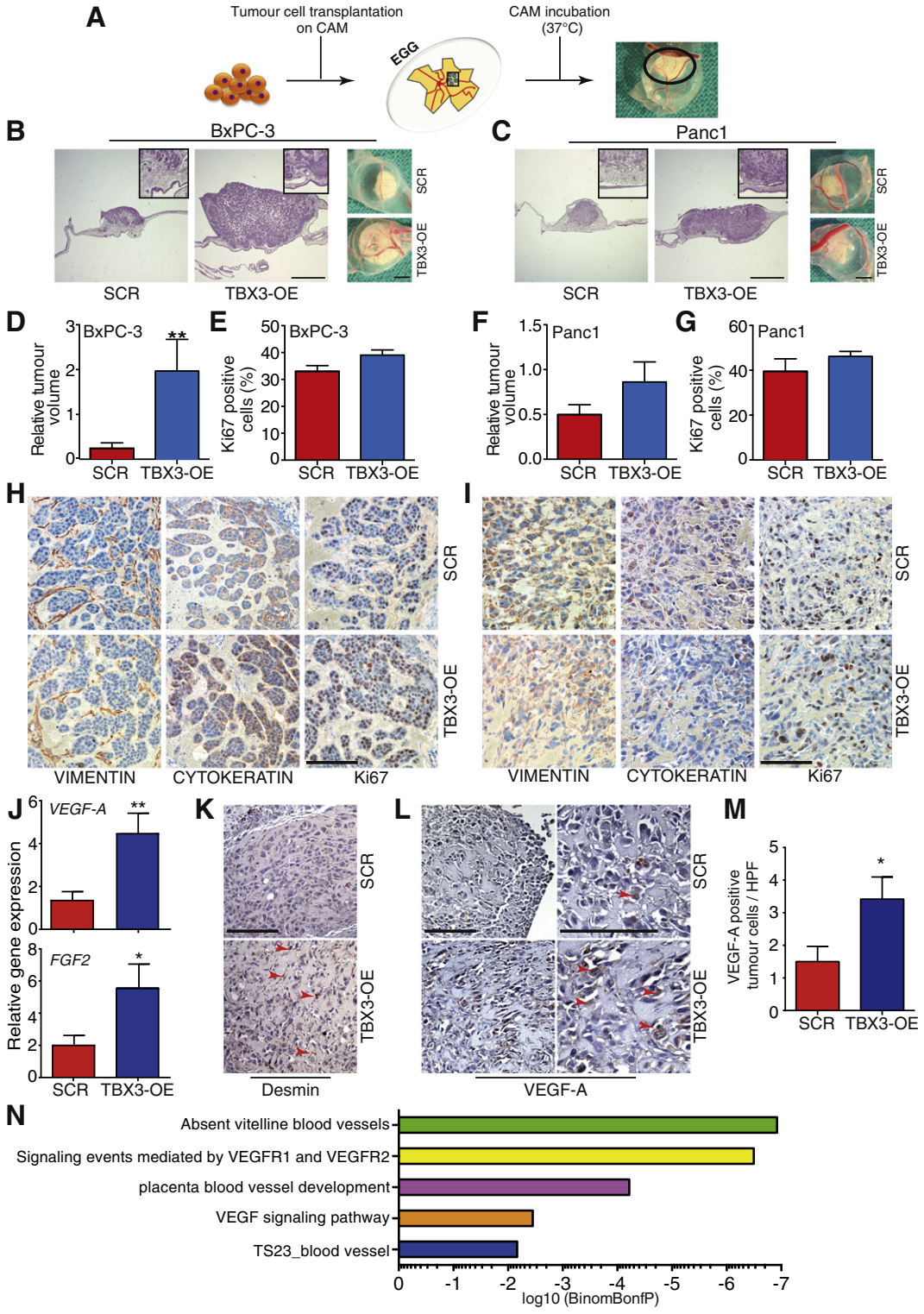

Fig. 3. TBX3 increases tumour growth *in vivo*. (A) Schematic description of the Chick Chorio Allantoic Membrane (CAM) assay. A total of 10^6 cells (BxPC3, Panc1) were applied per CAM and incubated for 72 h before analysis. Representative pictures of the CAM assays after explantation depicts notably increased tumour volumes and vascularization in (B) BxPC3 and (C) Panc1 TBX3-OE cells. Scale bar: 2 mm. Representative H&E stainings are provided in the lower panel. Scale bar: 1 mm. (D,F) TBX3 overexpression results in more extensive tumour growth with increased locally scattered tumour islets (inserts B, C). (E, G) Immunohistochemistry for Ki67 reveals no significant differences between the groups. (H, I) Representative immunohistochemistry pictures from the explanted tumours. Scale bar: 20 μm. Vimentin and Cytokeratin stainings show no differences between SCR and TBX3-OE in BxPC3 (H) and Panc1 cells (I). (n ≥ 4 eggs per group). (J) qRT-PCR analysis of *FGF2* and *VEGF-A* expression, showing increased levels of vascular markers in TBX3-OE tumour lines. Data are represented as relative gene expression of *FGF2* and *VEGF-A* and normalized to *HMBS*. Immunohistochemistry staining for (K) Desmin and (L) VEGF-A as an illustration of vascular tissue. Scale bar: 20 μm. (M) Quantification of VEGF positive structures per 5 high power fields per CAM. (N) Genomic Regions Enrichment of Annotations Tool (GREAT) (http://great.stanford.edu/public/html/index.php) analysis: Listed are all enriched GO terms in TBX3 bound genes with either "VEGFR1/-2", "blood vessel development", "VEGF signalling pathway" in their description.

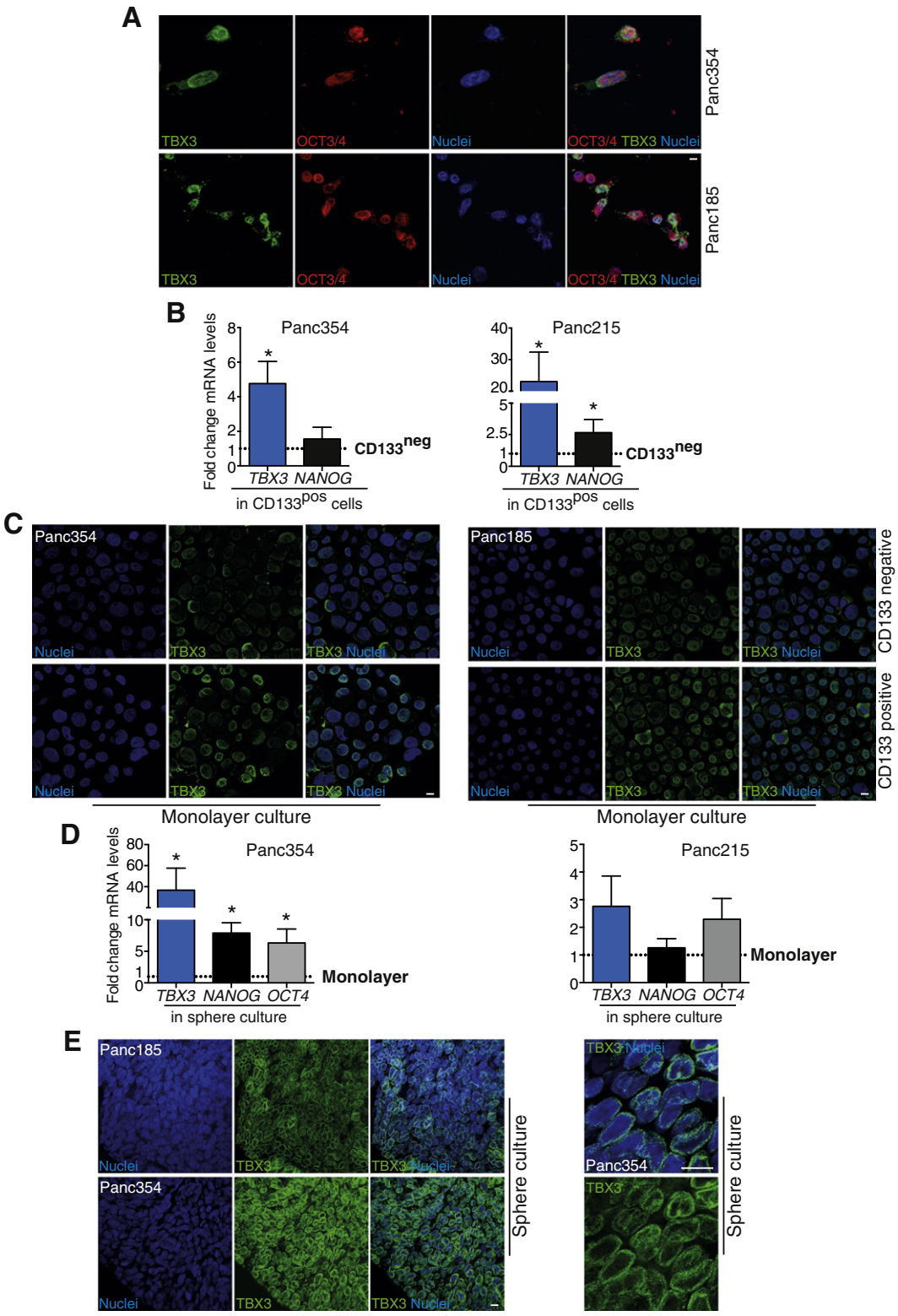

Fig. 4. TBX3 co-localizes with OCT3/4 in human PDAC cells and is highly expressed within a CD133^{+} subpopulation and tumour spheres. (A) Co-localization of TBX3 and OCT3/4 in monolayer cultures from two primary PDAC cell lines (Panc354 and Panc185). TBX3 (green), OCT3/4 (red), Nuclei-DAPI (blue), 63× magnification. Scale bar: 10 μm (B) *TBX3* and *NANOG* are significantly upregulated in sorted CD133^{+} versus CD133^{-} Panc354 (left) and Panc215 (right) primary PDAC cell lines. Data are normalized to *HPRT* and are presented as fold change relative to CD133^{-} cells. (C) Immunofluorescence stainings of CD133^{+}/CD133^{-} PDAC cells (re-plated and cultured under monolayer conditions): High expression of TBX3 on protein level in CD133^{+} cells while TBX3 is virtually absent in the CD133^{-} population. TBX3 (green), Nuclei DAPI (blue) (Panc354 and Panc185). Scale bar: 10 μm (D) qRT-PCR analysis shows upregulation of *TBX3* and the pluripotency-associated genes *NANOG* and *OCT4* in CSC-enriched spheres as compared to monolayer cultures (E) Illustration of TBX3 Expression in tumour spheres from a primary PDAC cell line (Panc354 and Panc185): TBX3 (green), Nuclei DAPI (blue), 63× magnification. Scale bar: 10 μm.

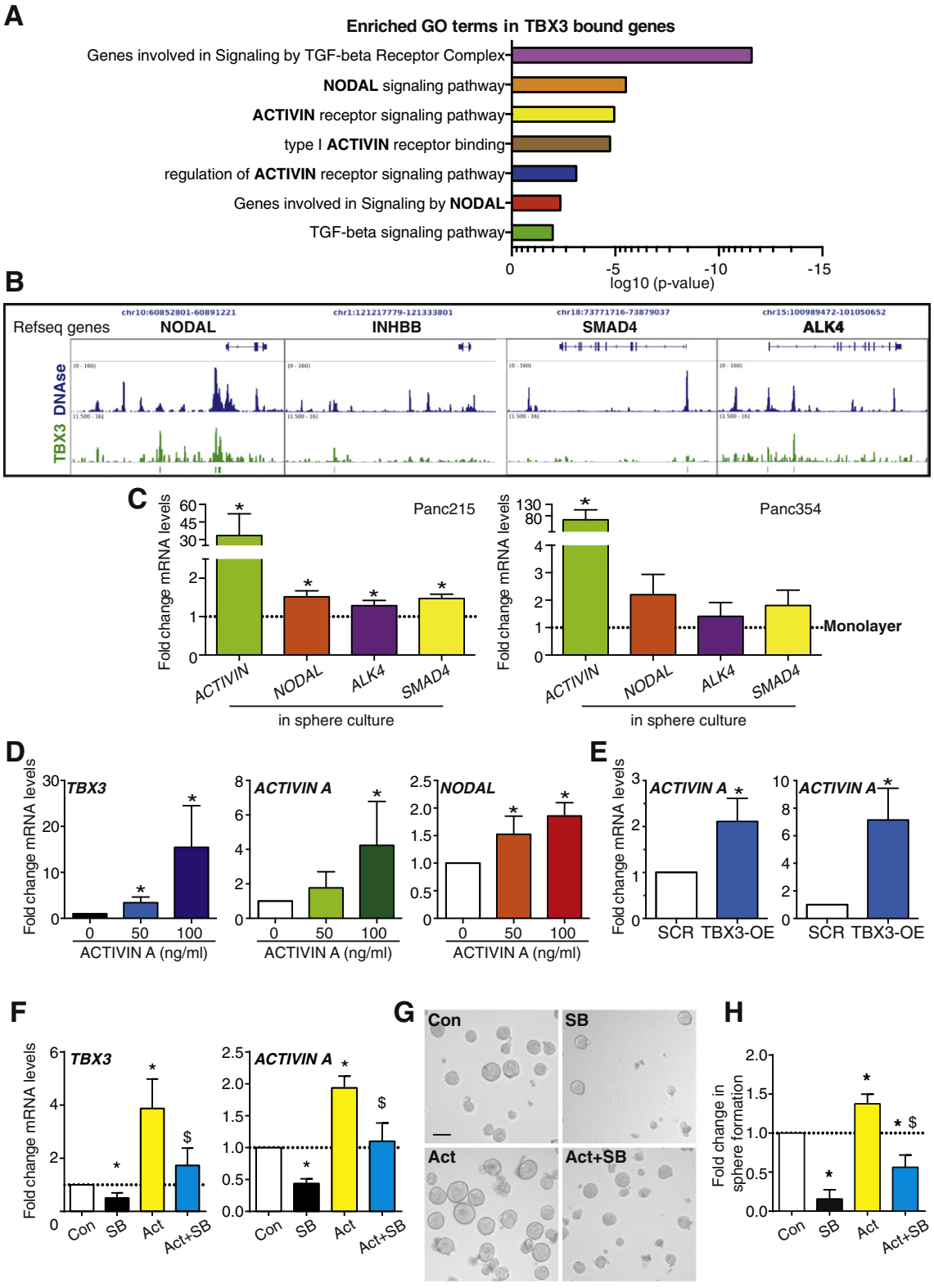

Fig. 5. TBX3 induces a cancer stem cell phenotype in primary pancreatic cancer cells. (A) Listed are the terms referring to "Nodal-, TGF-b- and Activin-signalling" out of the top enriched GO terms using a gene-based enrichment analysis with the GREAT tool of the genes that possess a TBX3 binding peak in mouse embryonic stem cells (Waghray et al., 2015). (B) ChIP-Seq profiles of TBX3 in mouse embryonic stem cells around NODAL, INHBB, SMAD4 and ALK4 genes. (C) NODAL/ACTIVIN signalling pathway members are increased in sphere cultures of Panc215 (left) and Panc354 (right) cells on mRNA levels. (D) Expression of *TBX3* and *ACTIVIN A* and *NODAL* is upregulated in a dose-dependent manner after stimulation of Panc354 cells with ACTIVIN A. (E) *ACTIVIN A* mRNA expression is significantly increased upon overexpression of TBX3 in BxPC3 cells (left) and Panc354 cells (right). (F) Treatment with SB431542 (SB), a selective inhibitor of Activin Receptor-like Kinase Receptors (ALKs), leads to a significant reduction of *TBX3* and *Activin A* expression in spheres from a primary tumour cell line. (n ≥ 3 for all experiments, dotted lines indicate respective control) (G) Visible Reduction of sphere formation capability in a primary tumour cell line after treatment with SB. Scale bar: 100 μm. (H) Relative quantification of tumour spheres upon treatment with SB. mRNA data is presented as fold change in relation to monolayer control.

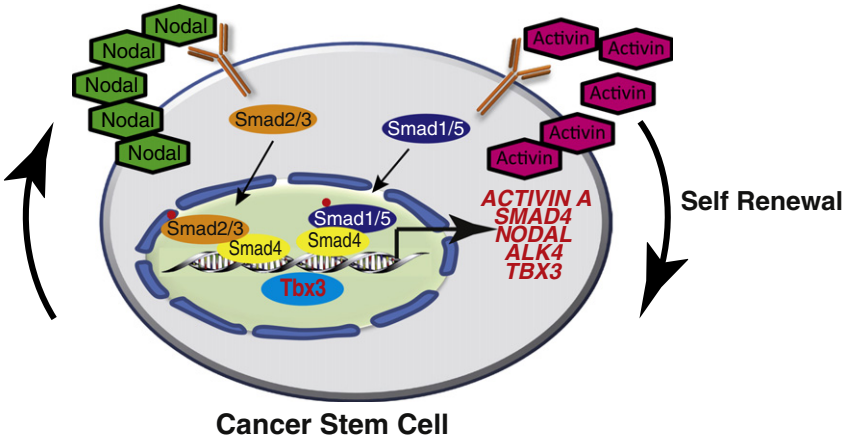

Fig. 6. Schematic model of an autocrine NODAL/ACTIVIN–TBX3–NODAL/ACTIVIN loop in human pancreatic cancer stem cells.

proliferation in some tumours (Peres et al., 2010). In contrast to TBX3, TBX2 is a well-known inducer of proliferation, and is known to be a downstream target of TBX3 (Muller et al., 2012). One could hypothesize that the lack of proliferation may result from a direct inhibition of TBX2 as a result of TBX3 overexpression. Furthermore, others have already shown TBX3 to be a key mediator for TGFβ1 signalling, thus negatively regulating proliferation and inducing migration and invasion (Li et al., 2013). On the other hand, we detected a significantly increased migratory and invasive capacity in different PDAC cell lines that depended on TBX3 expression.

In CAM assays as an *in vivo* platform to study tumorigenic potential, TBX3 overexpression resulted in a significantly increased tumour formation capacity and consecutively larger tumours, which almost penetrated the CAM. This is well in line with our *in vitro* data showing increased migration and invasion, and is supported by the role of TBX3 in malignant melanoma, where it drives invasiveness (Peres and Prince, 2013). Of note, previous reports describe TBX3-dependent down-regulation of E-cadherin (Boyd et al., 2013), which is recognized as a crucial step during EMT and subsequent metastatic spread of tumours (Vanharanta and Massague, 2013). While we made similar observations in CAM tumours as suggested by immunohistochemistry and qPCR, we were unable to detect TBX3-mediated induction of EMT *in vitro*. Neither the epithelial BxPC3 nor the more mesenchymal Panc1 cells showed a TBX3-dependent regulation of EMT marker genes. This might be in line with recent reports showing that EMT is dispensable for metastasis but induces chemoresistance in pancreatic cancer (Zheng et al., 2015), and further supports our dataset where challenging cell culture with low serum, hypoxia or chemotherapy showed no TBX3-dependent effects.

Another explanation for the increased tumour formation might by the higher intrinsic tumour-initiating capacity of TBX3 overexpressing cells and a TBX3-related induction of angiogenesis, which we found to be elevated after TBX3 overexpression. Since we have shown previously that TBX3 is critically involved in the self-renewal and the pluripotency of induced pluripotent stem cells (iPSCs) (Weidgang et al., 2013; Russell et al., 2015b), the regulation of a "stemness" phenotype together with the observation of increased aggressiveness in tumour formation led us to investigate whether TBX3 serves as a mediator of a cancer stem cell phenotype in pancreatic cancer. Using sphere formation as an established surrogate assay for self-renewal *in vitro*, the overexpression of TBX3 resulted in significantly enhanced sphere formation. Moreover, TBX3 is highly expressed within spheres. Pancreatic cancer stem cells are usually enriched by sorting for surface markers such as CD133 (Hermann et al., 2007) or CD44/CD24/EpCAM (Li et al., 2007), or in sphere cultures that promote the survival and expansion of undifferentiated cells in anchorage-independent conditions. Neither approach identifies a pure population, and surface markers have been under intense debate since they may vary considerably on inter-individual differences between patients, (chemo-)therapies, culture techniques, and utilized antibodies (Wicha, 2006). TBX3 is indeed overexpressed in $CD133^{+}$ cells and sphere cultures. We therefore proceeded to investigate the functional role of TBX3 in CSCs. We have shown previously that TBX3 reinforces an autocrine TBX3–NODAL–SMAD2 signalling loop to mediate mesendodermal differentiation in embryonic stem cells (Weidgang et al., 2013; Russell et al., 2015b; Weidgang et al., 2016). The signalling pathways shared between embryonic stem cells and cancer cells prompted us to use a recent TBX3 ChIP-sequencing dataset to identify putative self-renewal pathways in CSCs. Not only did we identify key signalling networks for the self-renewal of pancreatic CSCs such as TGFB, NODAL and ACTIVIN signalling, but we also validated these findings in a set of core genes previously described to be highly relevant in these processes. Interestingly, the endogenous overexpression of TBX3 induces *NODAL* and *ACTIVIN*, whereas exogenous treatment with recombinant ACTIVIN induces *TBX3* expression. This autocrine feedback loop is most likely responsible for the self-renewal of CSCs. Pharmacological inhibition of key ACTIVIN receptors (ALKs 4/5) repressed key effects of the TBX3–NODAL–SMAD2 signalling loop such as gene expression and sphere formation. We have shown previously that NODAL/ACTIVIN signalling is active in CSCs and that it is critical for their perpetuation and tumorigenic potential (Lonardo et al., 2011). Previous studies have already provided evidence for NODAL/ACTIVIN-induced angiogenesis: (i) inhibition of ALK-4 reduces tumour-angiogenesis in breast cancer cell lines (Siragam et al., 2012) and (ii) Smad2/Smad3 pathway activation mediated by ALK4 and ALK5 activates Growth Differentiation Factor 11 (GDF11)–induced migration and angiogenesis in endothelial progenitor cells (Williams et al., 2013). This newly postulated mechanism deserves further investigation in PDAC, since we could demonstrate a relevant induction of both VEGF-expression in PDAC cells after TBX3 overexpression and an increase in VEGF and FGF-2 positive vascular structures in the CAM-assay.

Furthermore, we have identified the tumour stroma, and pancreatic stellate cells in particular, to be an abundant source of NODAL and ACTIVIN, thus creating a supportive niche for these highly plastic cells (Lonardo et al., 2012). Since pancreatic cancers are usually highly desmoplastic tumours which are characterized by extensive infiltration of stromal cells, paracrine NODAL/ACTIVIN secreted by stellate cells and TGFβ secreted by CSCs seem to be critical for the perpetuation of CSCs, and interference with this cross-stimulation seems to be highly relevant for successful therapy (Lonardo et al., 2011; Lonardo et al., 2012). Accordingly, a miR-19-72 cluster that has been shown to regulate TBX3 expression confers a cancer stem cell phenotype to non-CSCs (Cioffi et al., 2015).

In summary, we here identify a new TBX3-dependent autocrine stimulation loop through which CSCs can regulate NODAL/ACTIVIN

signalling in the absence of stromal cells. This leads to increased migratory and invasive properties in the tumour, and drives a cancer stem cell population involving an autocrine positive feedback regulation of the NODAL/ACTIVIN–TBX3–NODAL/ACTIVIN axis. This establishes TBX3 as a new key player in cells with cancer stem cell features, and gives a new mechanistic angle to previous successful approaches for the elimination of CSCs and subsequently improved therapy against pancreatic cancer.

Conflict of interest

None

The following are the supplementary data related to this article

Supplementary data to this article can be found online at http://dx.doi.org/10.1016/j.scr.2016.08.007.

Acknowledgement

We are indebted to Claudia Ruhland and Claudia Längle their excellent technical support. We thank Daniel Hartmann for providing mRNA from normal pancreas and PDAC samples. This study was funded by the Deutsche Forschungsgemeinschaft (DFG, K.L. 2544/1-1 and 1-2), the Forschungskern SyStaR to A.K., BIU (Böhringer Ingelheim Ulm to A.K.), the Else-Kröner-Fresenius-Stiftung (2011_A200), a German Cancer Aid Max Eder Fellowship to P.C.H., a German Cancer Aid Grant to A.K. (111879), the Fritz-Thyssen Foundation to A.K. (2015-00363) and the Hector Foundation Cancer Research Fund to P.C.H. A.K. is indebted to the Baden-Württemberg Stiftung for the financial support of this research project by the Eliteprogramme for Postdocs. A.K. is also an Else-Kröner-Fresenius Memorial Fellow. This work was also supported by the Interdisciplinary Center for Clinical Research (IZKF Aachen), RWTH Aachen University Medical School, Aachen, Germany to I.G.C. The Else Kröner-Forschungskolleg Ulm supports L.P.M.H. receives funding from the Bausteinprogramm of Ulm University. We thank Dr. Ronan Russell for generating some of the Tbx3 gain of function cell lines and for supporting us with the CAM experiments and intellectual input.

References

Al-Hajj, M., Wicha, M.S., Benito-Hernandez, A., Morrison, S.J., Clarke, M.F., 2003. Prospective identification of tumorigenic breast cancer cells. Proc. Natl. Acad. Sci. USA 100, 3983–3988.

Amir, S., Simion, C., Umeh-Garcia, M., Krig, S., Moss, T., Carraway 3rd, K.L., Sweeney, C., 2016. Regulation of the T-box transcription factor Tbx3 by the tumour suppressor microRNA-206 in breast cancer. Br. J. Cancer 114, 1125–1134.

Azoitei, N., Pusapati, G.V., Kleger, A., Moller, P., Kufer, R., Genze, F., Wagner, M., van Lint, J., Carmeliet, P., Adler, G., Seufferlein, T., 2010. Protein kinase D2 is a crucial regulator of tumour cell-endothelial cell communication in gastrointestinal tumours. Gut 59, 1316–1330.

Azoitei, N., Kleger, A., Schoo, N., Thal, D.R., Brunner, C., Pusapati, G.V., Filatova, A., Genze, F., Moller, P., Acker, T., Kuefer, R., Van Lint, J., Baust, H., Adler, G., Seufferlein, T., 2011. Protein kinase D2 is a novel regulator of glioblastoma growth and tumor formation. Neuro-Oncology 13, 710–724.

Azoitei, N., Hoffmann, C.M., Ellegast, J.M., Ball, C.R., Obermayer, K., Gossele, U., Koch, B., Faber, K., Genze, F., Schrader, M., Kestler, H.A., Dohner, H., Chiosis, G., Glimm, H., Frohling, S., Scholl, C., 2012. Targeting of KRAS mutant tumors by HSP90 inhibitors involves degradation of STK33. J. Exp. Med. 209, 697–711.

Azoitei, N., Diepold, K., Brunner, C., Rouhi, A., Genze, F., Becher, A., Kestler, H., van Lint, J., Chiosis, G., Koren 3rd, J., Frohling, S., Scholl, C., Seufferlein, T., 2014. HSP90 supports tumor growth and angiogenesis through PRKD2 protein stabilization. Cancer Res. 74, 7125–7136.

Bertolessi, M., Linta, L., Seufferlein, T., Kleger, A., Liebau, S., 2015. A fresh look on T-box factor action in early embryogenesis (T-box factors in early development). Stem Cells Dev. 24, 1833–1851.

Beukers, W., Kandimalla, R., Masius, R.G., Vermeij, M., Kranse, R., van Leenders, G.J., Zwarthoff, E.C., 2015. Stratification based on methylation of TBX2 and TBX3 into three molecular grades predicts progression in patients with pTa-bladder cancer. Mod. Pathol. 28, 515–522.

Boyd, S.C., Mijatov, B., Pupo, G.M., Tran, S.L., Gowrishankar, K., Shaw, H.M., Goding, C.R., Scolyer, R.A., Mann, G.J., Kefford, R.F., Rizos, H., Becker, T.M., 2013. Oncogenic B-RAF(V600E) signaling induces the T-Box3 transcriptional repressor to repress E-cadherin and enhance melanoma cell invasion. J. Invest. Dermatol. 133, 1269–1277.

Burgucu, D., Guney, K., Sahinturk, D., Ozbudak, I.H., Ozel, D., Ozbilim, G., Yavuzer, U., 2012. Tbx3 represses PTEN and is over-expressed in head and neck squamous cell carcinoma. BMC Cancer 12, 481.

Cioffi, M., Trabulo, S.M., Sanchez-Ripoll, Y., Miranda-Lorenzo, I., Lonardo, E., Dorado, J., Reis Vieira, C., Ramirez, J.C., Hidalgo, M., Aicher, A., Hahn, S., Sainz Jr., B., Heeschen, C., 2015. The miR-17-92 cluster counteracts quiescence and chemoresistance in a distinct subpopulation of pancreatic cancer stem cells. Gut 64, 1936–1948.

Ciriello, G., Gatza, M.L., Beck, A.H., Wilkerson, M.D., Rhie, S.K., Pastore, A., Zhang, H., McLellan, M., Yau, C., Kandoth, C., Bowlby, R., Shen, H., Hayat, S., Fieldhouse, R., Lester, S.C., Tse, G.M., Factor, R.E., Collins, L.C., Allison, K.H., Chen, Y.Y., Jensen, K., Johnson, N.B., Oesterreich, S., Mills, G.B., Cherniack, A.D., Robertson, G., Benz, C., Sander, C., Laird, P.W., Hoadley, K.A., King, T.A., Network, T.R., Perou, C.M., 2015. Comprehensive molecular portraits of invasive lobular breast cancer. Cell 163, 506–519.

Eiseler, T., Kohler, C., Nimmagadda, S.C., Jamali, A., Funk, N., Joodi, G., Storz, P., Seufferlein, T., 2012. Protein kinase D1 mediates anchorage-dependent and -independent growth of tumor cells via the zinc finger transcription factor Snail1. J. Biol. Chem. 287, 32367–32380.

Fan, W., Huang, X., Chen, C., Gray, J., Huang, T., 2004. TBX3 and its isoform TBX3 + 2a are functionally distinctive in inhibition of senescence and are overexpressed in a subset of breast cancer cell lines. Cancer Res. 64, 5132–5139.

Fillmore, C.M., Gupta, P.B., Rudnick, J.A., Caballero, S., Keller, P.J., Lander, E.S., Kuperwasser, C., 2010. Estrogen expands breast cancer stem-like cells through paracrine FGF/Tbx3 signaling. Proc. Natl. Acad. Sci. U. S. A. 107, 21737–21742.

Fischer, K., Pflugfelder, G.O., 2015. Putative breast cancer driver mutations in TBX3 cause impaired transcriptional repression. Front. Oncol. 5, 244.

Gadaleta, E., Cutts, R.J., Kelly, G.P., Crnogorac-Jurcevic, T., Kocher, H.M., Lemoine, N.R., Chelala, C., 2011. A global insight into a cancer transcriptional space using pancreatic data: importance, findings and flaws. Nucleic Acids Res. 39, 7900–7907.

Haberland, J., Bertz, J., Wolf, U., Ziese, T., Kurth, B.M., 2010. German cancer statistics 2004. BMC Cancer 10, 52.

Haeno, H., Gonen, M., Davis, M.B., Herman, J.M., Iacobuzio-Donahue, C.A., Michor, F., 2012. Computational modeling of pancreatic cancer reveals kinetics of metastasis suggesting optimum treatment strategies. Cell 148, 362–375.

Hermann, P.C., Huber, S.L., Herrler, T., Aicher, A., Ellwart, J.W., Guba, M., Bruns, C.J., Heeschen, C., 2007. Distinct populations of cancer stem cells determine tumor growth and metastatic activity in human pancreatic cancer. Cell Stem Cell 1 (3), 313–323.

Hermann, P.C., Huber, S.L., Heeschen, C., 2008. Metastatic cancer stem cells: a new target for anti-cancer therapy? Cell Cycle 7, 188–193.

Hermann, P.C., Trabulo, S.M., Sainz Jr., B., Balic, A., Garcia, E., Hahn, S.A., Vandana, M., Sahoo, S.K., Tunici, P., Bakker, A., Hidalgo, M., Heeschen, C., 2013. Multimodal treatment eliminates cancer stem cells and leads to long-term survival in primary human pancreatic cancer tissue xenografts. PLoS ONE 8, e66371.

Howlader, N., Krapcho, M., et al., 2013. SEER Cancer Statistics Review, 1975–2011, National Cancer Institute, SEER Web Site,.

Jemal, A., Siegel, R., Xu, J., Ward, E., 2010. Cancer statistics, 2010. CA Cancer J. Clin. 60, 277–300.

Kartikasari, A.E., Zhou, J.X., Kanji, M.S., Chan, D.N., Sinha, A., Grapin-Botton, A., Magnuson, M.A., Lowry, W.E., Bhushan, A., 2013. The histone demethylase Jmjd3 sequentially associates with the transcription factors Tbx3 and Eomes to drive endoderm differentiation. EMBO J. 32, 1393–1408.

Kim, C.F., Jackson, E.L., Woolfenden, A.E., Lawrence, S., Babar, I., Vogel, S., Crowley, D., Bronson, R.T., Jacks, T., 2005. Identification of bronchioalveolar stem cells in normal lung and lung cancer. Cell 121, 823–835.

Kim, J., Chu, J., Shen, X., Wang, J., Orkin, S.H., 2008. An extended transcriptional network for pluripotency of embryonic stem cells. Cell 132, 1049–1061.

Kleger, A., Seufferlein, T., Malan, D., Tischendorf, M., Storch, A., Wolheim, A., Latz, S., Protze, S., Porzner, M., Proepper, C., Brunner, C., Katz, S.F., Pusapati, G.V., Bullinger, L., Franz, W.M., Koehntop, R., Giehl, K., Spyrantis, A., Wittekindt, O., Lin, Q., Zenke, M., Fleischmann, B.K., Wartenberg, M., Wobus, A.M., Boeckers, T.M., Liebau, S., 2010. Modulation of calcium-activated potassium channels induces cardiogenesis of pluripotent stem cells and enrichment of pacemaker-like cells. Circulation 122, 1823–1836.

Kleger, A., Mahaddalkar, P.U., Katz, S.F., Lechel, A., Joo, J.Y., Loya, K., Lin, Q., Hartmann, D., Liebau, S., Kraus, J.M., Cantz, T., Kestler, H.A., Zaehres, H., Scholer, H., Rudolph, K.L., 2012. Increased reprogramming capacity of mouse liver progenitor cells, compared with differentiated liver cells, requires the BAF complex. Gastroenterology 142, 907–917.

Li, H., Durbin, R., 2009. Fast and accurate short read alignment with Burrows-Wheeler transform. Bioinformatics 25, 1754–1760.

Li, C., Heidt, D.G., Dalerba, P., Burant, C.F., Zhang, L., Adsay, V., Wicha, M., Clarke, M.F., Simeone, D.M., 2007. Identification of pancreatic cancer stem cells. Cancer Res. 67, 1030–1037.

Li, J., Weinberg, M.S., Zerbini, L., Prince, S., 2013. The oncogenic TBX3 is a downstream target and mediator of the TGF-beta1 signaling pathway. Mol. Biol. Cell 24, 3569–3576.

Liebau, S., Stockmann, M., Illing, A., Seufferlein, T., Kleger, A., 2014. Induced pluripotent stem cells. A new resource in modern medicine. Internist 55, 460–469.

Lonardo, E., Hermann, P.C., Mueller, M.T., Huber, S., Balic, A., Miranda-Lorenzo, I., Zagorac, S., Alcala, S., Rodriguez-Arabaolaza, I., Ramirez, J.C., Torres-Ruiz, R., Garcia, E., Hidalgo, M., Cebrian, D.A., Heuchel, R., Lohr, M., Berger, F., Bartenstein, P., Aicher, A., Heeschen, C., 2011. Nodal/activin signaling drives self-renewal and tumorigenicity of pancreatic cancer stem cells and provides a target for combined drug therapy. Cell Stem Cell 9, 433–446.

Lonardo, E., Frias-Aldeguer, J., Hermann, P.C., Heeschen, C., 2012. Pancreatic stellate cells form a niche for cancer stem cells and promote their self-renewal and invasiveness. Cell Cycle 11, 1282–1290.

Minguillon, C., Logan, M., 2003. The comparative genomics of T-box genes. Brief. Funct. Genomic. Proteomic. 2, 224–233.

Mowla, S., Pinnock, R., Leaner, V.D., Goding, C.R., Prince, S., 2011. PMA-induced up-regulation of TBX3 is mediated by AP-1 and contributes to breast cancer cell migration. Biochem. J. 433, 145–153.

Mueller, M.T., Hermann, P.C., Witthauer, J., Rubio-Viqueira, B., Leicht, S.F., Huber, S., Ellwart, J.W., Mustafa, M., Bartenstein, P., D'Haese, J.G., Schoenberg, M.H., Berger, F., Jauch, K.W., Hidalgo, M., Heeschen, C., 2009. Combined targeted treatment to eliminate tumorigenic cancer stem cells in human pancreatic cancer. Gastroenterology 137, 1102–1113.

Muller, C.W., Herrmann, B.G., 1997. Crystallographic structure of the T domain-DNA complex of the Brachyury transcription factor. Nature 389, 884–888.

Muller, M., Stockmann, M., Malan, D., Wolheim, A., Tischendorf, M., Linta, L., Katz, S.F., Lin, Q., Latz, S., Brunner, C., Wobus, A.M., Zenke, M., Wartenberg, M., Boeckers, T.M., von Wichert, G., Fleischmann, B.K., Liebau, S., Kleger, A., 2012. Ca2+ activated K channels-new tools to induce cardiac commitment from pluripotent stem cells in mice and men. Stem Cell Rev. 8, 720–740.

Muller, M., Schroer, J., Azoitei, N., Eiseler, T., Bergmann, W., Kohntop, R., Lin, Q., Costa, I.G., Zenke, M., Genze, F., Weidgang, C., Seufferlein, T., Liebau, S., Kleger, A., 2015. A time frame permissive for protein kinase D2 activity to direct angiogenesis in mouse embryonic stem cells. Sci. Rep. 5, 11742.

O'Brien, C.A., Pollett, A., Gallinger, S., Dick, J.E., 2007. A human colon cancer cell capable of initiating tumour growth in immunodeficient mice. Nature 445, 106–110.

Peres, J., Prince, S., 2013. The T-box transcription factor, TBX3, is sufficient to promote melanoma formation and invasion. Mol. Cancer 12, 117.

Peres, J., Davis, E., Mowla, S., Bennett, D.C., Li, J.A., Wansleben, S., Prince, S., 2010. The highly homologous T-box transcription factors, TBX2 and TBX3, have distinct roles in the oncogenic process. Genes Cancer 1, 272–282.

Rahib, L., Smith, B.D., Aizenberg, R., Rosenzweig, A.B., Fleshman, J.M., Matrisian, L.M., 2014. Projecting cancer incidence and deaths to 2030: the unexpected burden of thyroid, liver, and pancreas cancers in the United States. Cancer Res. 74, 2913–2921.

Renard, C.A., Labalette, C., Armengol, C., Cougot, D., Wei, Y., Cairo, S., Pineau, P., Neuveut, C., de Reynies, A., Dejean, A., Perret, C., Buendia, M.A., 2007. Tbx3 is a downstream target of the Wnt/beta-catenin pathway and a critical mediator of beta-catenin survival functions in liver cancer. Cancer Res. 67, 901–910.

Rhim, A.D., Mirek, E.T., Aiello, N.M., Maitra, A., Bailey, J.M., McAllister, F., Reichert, M., Beatty, G.L., Rustgi, A.K., Vonderheide, R.H., Leach, S.D., Stanger, B.Z., 2012. EMT and dissemination precede pancreatic tumor formation. Cell 148, 349–361.

Ricci-Vitiani, L., Lombardi, D.G., Pilozzi, E., Biffoni, M., Todaro, M., Peschle, C., De Maria, R., 2007. Identification and expansion of human colon-cancer-initiating cells. Nature 445, 111–115.

Rubio-Viqueira, B., Hidalgo, M., 2009. Direct in vivo xenograft tumor model for predicting chemotherapeutic drug response in cancer patients. Clin. Pharmacol. Ther. 85, 217–221.

Russell, R., Perkhofer, L., Liebau, S., Lin, Q., Lechel, A., Feld, F.M., Hessmann, E., Gaedcke, J., Guthle, M., Zenke, M., Hartmann, D., von Figura, G., Weissinger, S.E., Rudolph, K.L., Moller, P., Lennerz, J.K., Seufferlein, T., Wagner, M., Kleger, A., 2015a. Loss of ATM accelerates pancreatic cancer formation and epithelial-mesenchymal transition. Nat. Commun. 6, 7677.

Russell, R., Ilg, M., Lin, Q., Wu, G., Lechel, A., Bergmann, W., Eiseler, T., Linta, L., Kumar, P.P., Klingenstein, M., Adachi, K., Hohwieler, M., Sakk, O., Raab, S., Moon, A., Zenke, M., Seufferlein, T., Schöler, H.R., Illing, A., Liebau, S., Kleger, A., 2015b. A dynamic role of TBX3 in the pluripotency circuitry. Stem Cell Rep.

Sancho, P., Burgos-Ramos, E., Tavera, A., Bou Kheir, T., Jagust, P., Schoenhals, M., Barneda, D., Sellers, K., Campos-Olivas, R., Grana, O., Viera, C.R., Yuneva, M., Sainz Jr., B., Heeschen, C., 2015. MYC/PGC-1alpha balance determines the metabolic phenotype and plasticity of pancreatic cancer stem cells. Cell Metab. 22, 590–605.

Shan, Z.Z., Yan, X.B., Yan, L.L., Tian, Y., Meng, Q.C., Qiu, W.W., Zhang, Z., Jin, Z.M., 2015. Overexpression of Tbx3 is correlated with epithelial-mesenchymal transition phenotype and predicts poor prognosis of colorectal cancer. Am. J. Cancer Res. 5, 344–353.

Singh, S.K., Hawkins, C., Clarke, I.D., Squire, J.A., Bayani, J., Hide, T., Henkelman, R.M., Cusimano, M.D., Dirks, P.B., 2004. Identification of human brain tumour initiating cells. Nature 432, 396–401.

Siragam, V., Rutnam, Z.J., Yang, W., Fang, L., Luo, L., Yang, X., Li, M., Deng, Z., Qian, J., Peng, C., Yang, B.B., 2012. MicroRNA miR-98 inhibits tumor angiogenesis and invasion by targeting activin receptor-like kinase-4 and matrix metalloproteinase-11. Oncotarget 3, 1370–1385.

Vanharanta, S., Massague, J., 2013. Origins of metastatic traits. Cancer Cell 24, 410–421.

Waghray, A., Saiz, N., Jayaprakash, A.D., Freire, A.G., Papatsenko, D., Pereira, C.F., Lee, D.F., Brosh, R., Chang, B., Darr, H., Gingold, J., Kelley, K., Schaniel, C., Hadjantonakis, A.K., Lemischka, I.R., 2015. Tbx3 controls Dppa3 levels and exit from pluripotency toward mesoderm. Stem Cell Rep. 5, 97–110.

Wang, H.C., Meng, Q.C., Shan, Z.Z., Yuan, Z., Huang, X.Y., 2015. Overexpression of Tbx3 predicts poor prognosis of patients with resectable pancreatic carcinoma. Asian Pac. J. Cancer Prev. 16, 1397–1401.

Weidgang, C.E., Russell, R., Tata, P.R., Kuhl, S.J., Illing, A., Muller, M., Lin, Q., Brunner, C., Boeckers, T.M., Bauer, K., Kartikasari, A.E., Guo, Y., Radenz, M., Bernemann, C., Weiss, M., Seufferlein, T., Zenke, M., Iacovino, M., Kyba, M., Scholer, H.R., Kuhl, M., Liebau, S., Kleger, A., 2013. TBX3 directs cell-fate decision toward mesendoderm. Stem Cell Rep. 1, 248–265.

Weidgang, C.E., Seufferlein, T., Kleger, A., Mueller, M., 2016. Pluripotency actors on their lineage move. Stem Cells Int. 2016, 16.

Wicha, M.S., 2006. Cancer stem cells: an old idea–a paradigm shift. Cancer Res. 66, 1883–1890 (discussion 1895–1886).

Williams, G., Zentar, M.P., Gajendra, S., Sonego, M., Doherty, P., Lalli, G., 2013. Transcriptional basis for the inhibition of neural stem cell proliferation and migration by the TGFbeta-family member GDF11. PLoS ONE 8, e78478.

Willmer, T., Hare, S., Peres, J., Prince, S., 2016a. The T-box transcription factor TBX3 drives proliferation by direct repression of the p21(WAF1) cyclin-dependent kinase inhibitor. Cell Div 11, 6.

Willmer, T., Cooper, A., Sims, D., Govender, D., Prince, S., 2016b. The T-box transcription factor 3 is a promising biomarker and a key regulator of the oncogenic phenotype of a diverse range of sarcoma subtypes. Oncogenesis 5, e199.

Yachida, S., White, C.M., Naito, Y., Zhong, Y., Brosnan, J.A., Macgregor-Das, A.M., Morgan, R.A., Saunders, T., Laheru, D.A., Herman, J.M., Hruban, R.H., Klein, A.P., Jones, S., Velculescu, V., Wolfgang, C.L., Iacobuzio-Donahue, C.A., 2012. Clinical significance of the genetic landscape of pancreatic cancer and implications for identification of potential long-term survivors. Clin. Cancer Res. 18, 6339–6347.

Yarosh, W., Barrientos, T., Esmailpour, T., Lin, L., Carpenter, P.M., Osann, K., Anton-Culver, H., Huang, T., 2008. TBX3 is overexpressed in breast cancer and represses p14 ARF by interacting with histone deacetylases. Cancer Res. 68, 693–699.

Zhang, Y., Liu, T., Meyer, C.A., Eeckhoute, J., Johnson, D.S., Bernstein, B.E., Nusbaum, C., Myers, R.M., Brown, M., Li, W., Liu, X.S., 2008. Model-based analysis of ChIP-Seq (MACS). Genome Biol. 9, R137.

Zheng, X., Carstens, J.L., Kim, J., Scheible, M., Kaye, J., Sugimoto, H., Wu, C.C., LeBleu, V.S., Kalluri, R., 2015. Epithelial-to-mesenchymal transition is dispensable for metastasis but induces chemoresistance in pancreatic cancer. Nature 527, 525–530.